Adhesion and growth of human schwann cells on trimethylene carbonate (co)polymers

Ana Paula Pêgo,[1] Carmen L. A. M. Vleggeert-Lankamp,[2] Marga Deenen,[2] Egbert A. J. F. Lakke,[2] Dirk W. Grijpma,[1] André A. Poot,[1] Enrico Marani,[1,2] Jan Feijen[1]

[1]*Institute for Biomedical Technology (BMTI) and Department of Polymer Chemistry and Biomaterials, Faculty of Chemical Technology, University of Twente, P. O. Box 217, 7500 AE Enschede, The Netherlands*

[2]*Neuroregulation Group, Department of Neurosurgery, Leiden University Medical Center (LUMC), P. O. Box 9604, 2300 RC Leiden, The Netherlands*

Received 12 July 2002; accepted 11 February 2003

Abstract: Seeding of artificial nerve grafts with Schwann cells is a promising strategy for bridging large nerve defects. The aim of the present study was to evaluate the adhesion and growth of human Schwann cells (HSCs) on 1,3-trimethylene carbonate (TMC) and ϵ-caprolactone copolymers, with the final goal of using these materials in the development of an artificial nerve graft. The adhesion, proliferation, and morphology of HSCs on copolymers containing 10 and 82 mol % of TMC and on the parent homopolymers were investigated. HSCs adhered faster and in greater numbers on the copolymer with 82 mol % of TMC and on the TMC homopolymer compared with the other (co)polymers. On all polymer films, cell adhesion was lower than on gelatin (positive control). Despite differences in cell adhesion, cells displayed exponential growth on all tested surfaces, with similar growth rates. Cell numbers doubled approximately every 3 days on all substrates. When the polymer films were coated with fibronectin, no significant differences in cell adhesion and proliferation were observed between coated polymer surfaces and gelatin. The results indicate that all tested materials support the adhesion and proliferation of HSCs and can in principle be used for the preparation of flexible and slowly degrading nerve guides. © 2003 Wiley Periodicals, Inc. J Biomed Mater Res 67A: 876–885, 2003

Key words: poly(ester carbonate)s based on trimethylene carbonate and ϵ-caprolactone; human Schwann cells; cell adhesion and proliferation; fibronectin; degradable nerve guides

INTRODUCTION

Autologous nerve grafts are regarded as the "gold standard" for the repair of large peripheral nerve lesions. Nerve grafts can be placed between nerve fascicles, or more generally, between two severed nerve ends, providing a direct, unbroken path between nerve ends and preventing the ingrowth of scar tissue that might hinder nerve regeneration. However, the current technology is limited by donor tissue availability, secondary deformities, and possible mismatch in tissue organization and dimensions. An off-the-shelf artificial graft adaptable to the neurosurgeon's needs would be a welcome alternative in the treatment of nerve defects. The nerve conduit should preferably degrade after axonal regeneration to avoid an eventual late foreign-body response and chronic nerve compression that can jeopardize nerve recovery.[1]

The use of degradable artificial nerve guides has been extensively investigated *in vivo*.[2–7] But despite the many advances and contributions in the field of nerve tissue engineering, the results obtained with degradable nerve guides in the correction of large nerve defects have never reached the levels of nerve function recovery obtained with autologous nerve grafts.[8,9] Considering the graft material, the use of polymers with too high degradation rates, unsuitable mechanical properties, and impermeability of the device to body fluids have been listed as possible causes for graft failure.[10] Furthermore, a limited knowledge of the biochemical components and pathways involved in the nerve regeneration process might have prevented the successful selection of key elements for the regeneration process to be incorporated into the nerve guide.

In the past few years, much effort has been put into the identification of the factors involved in axonal regeneration. Outgrowth over clinically relevant dis-

Correspondence to: J. Feijen; e-mail: j.feijen@ct.utwente.nl

Contract grant sponsor: Portuguese Foundation for Science and Technology; contract grant number: BD/13335/97

tances and functional recovery seems to require additional stimulation by, for instance, contact with Schwann cells (SCs) and/or extracellular matrix (ECM) components. The incorporation of SCs into a nerve guide, with a few exceptions,[11] already proved to have a positive effect on the overall regeneration process, increasing peripheral nerve growth, myelination, and functional recovery.[12–17] These cells have a vital role in the natural nerve regeneration process, producing ECM proteins and a range of neurotropic and neurotrophic factors essential for neuron growth.[18–21]

Recently, we have published on the potential use of 1,3-trimethylene carbonate (TMC) and ϵ-caprolactone (CL)-based (co)polymers in the preparation of porous nerve conduits for bridging nerve gaps.[22] Poly(TMC) and TMC–CL copolymers with high CL content are very flexible and tough materials that can be processed into highly porous structures. These materials are biocompatible and their degradation rates can be tuned by adjusting the comonomer content.[23,24] The aim of the present study was to evaluate how variations in the polymer composition affect the adhesion, proliferation, and morphology of human SCs (HSCs) on TMC and CL (co)polymer substrates, with the final goal of using these materials in the preparation of artificial nerve grafts seeded with SCs.

Ultimately, the HSCs will be seeded on the inner surface of the graft either directly or after coating of the graft luminal surface with an adhesive protein.[25–27] Alternatively, the nerve guide can be filled with SCs in a supporting adhesive matrix.[12–14,17,28] Therefore, the effect of fibronectin coating of TMC and CL (co)polymers on the behavior of HSCs was also investigated.

MATERIALS AND METHODS

Materials

Unless indicated otherwise, all reagents and biochemicals were purchased from Sigma (St. Louis, MO). Solvents were of analytical grade (Biosolve, The Netherlands).

Polymer synthesis and characterization

The synthesis and characterization of the TMC (Boehringer Ingelheim, Germany) and CL (Acros Organics, Belgium) based polymers have been described in a previous study.[22] Briefly, the polymerizations were conducted by ring-opening polymerization in evacuated and sealed glass ampoules using stannous octoate as a catalyst. All homo- and copolymerizations were performed for a period of 3 days at 130°C. The obtained polymers were purified by dissolution in chloroform and subsequent precipitation into a 10-fold volume of isopropanol. The precipitated polymers were recovered, washed with fresh isopropanol, and dried under reduced pressure at room temperature until constant weight. The (co)polymer composition was determined by proton nuclear magnetic resonance (Varian Inova 300 MHz, Palo Alto, CA), the molecular weight by gel permeation chromatography (Waters, Milford, MA), and thermal properties were evaluated by means of differential scanning calorimetry (PerkinElmer Pyris 1, Norwalk, CT).

Preparation of polymer disks

Films were prepared by casting polymer solutions (4.0–6.5 wt/vol %) in chloroform onto glass plates. After drying the films under reduced pressure at room temperature, disks with a diameter of 17 mm were punched out.

The disks were sterilized by two incubation steps in 70 vol % ethanol solution for 15 min, followed by a rinsing step of 30 min in sterile water. After sterilization, individual disks were gently placed in wells of 24-well tissue culture plates (Costar, Cambridge, MA) and fixed with sterile rubber rings with a 15-mm internal diameter (Eriks, The Netherlands). After drying overnight in a laminar flow chamber, the disks were used for cell culture.

In selected experiments, sterilized disks were precoated by incubation at room temperature for 45 min with a 50-μg/mL human fibronectin solution (Roche Diagnostics, Germany) in phosphate buffered saline (PBS) (pH 7.4; NPBI, The Netherlands).

Characterization of polymer films

Static contact angles of ultra-pure water (MilliQ Plus; Millipore, France) on dry and wet polymer films and water uptake in PBS were used to evaluate the wettability of TMC and CL (co)polymers. Contact angle measurements based on the sessile drop (dry films) and captive bubble (wet films) methods were performed at room temperature using a video-based optical contact angle meter OCA 15 (DataPhysics Instruments GmbH, Germany). For the dry polymer surfaces, sessile drop contact angles were determined using films spin-coated from chloroform solutions (2 wt/vol %) onto glass slips (Menzel-Gläser, Germany) (readings were taken within the first 10–15 s). Contact angles of five different regions of each polymer film were measured and averaged. Contact angles of wet films were determined using the captive bubble method on 10-mm diameter disks punched out of the cast films, which were conditioned in ultra-pure water for 1 week. Contact angles of four different disks of each polymer were averaged.

The water uptake was defined as the weight gain of the polymer specimen after conditioning, according to:

$$\text{water uptake} = \frac{w - w_o}{w_o} \times 100\ (wt\%)$$

where w_o is the initial specimen weight and w the weight of the specimen after conditioning.

Compression-molded specimens were placed in PBS at 37°C and the weight change of the samples was evaluated until equilibrium was reached (within 24 h). Purified polymer samples 600-μm thick were compression molded at 140°C in a 100 × 50 × 0.6 mm^3 mold.

The surface structure of the films was evaluated using an S800 Field Emission scanning electron microscope (Hitachi, Japan) operating at 5 kV. Before scanning electron microscope analysis, samples were sputtered with a gold layer (Polaron, UK).

Isolation of HSCs

Pieces of sural nerve that remained after nerve transplantation to restore brachial plexus lesions in two patients were used to establish two HSC cultures (NCN61 and NCN68) by means of a sequential explantation technique.[29] All material was obtained from the Leiden University Medical Center (Department of Neurosurgery) after informed consent from the patients. After careful stripping of the epineurium and connective tissue, the sural nerve was cut into pieces of approximately 1 mm^3. These were placed in gelatin-coated culture flasks (Greiner, The Netherlands) and covered with a thin layer of LAK culture medium consisting of Dulbecco's modified Eagle's medium (Bio-Whittaker Europe, Belgium), 10% lymphokine activated killer cells conditioned medium (LAK),[30] 5% fetal calf serum (Gibco BRL, Life Technologies, Germany), 0.25 μL/mL phytohaema-agglutinin (Difco Laboratories, Detroit, MI), 100 IU/mL penicillin (Gist-Brocades, The Netherlands), and 50 μg/mL streptomycin (Gist-Brocades).

Gelatin coatings on the culture flasks were prepared by incubating a 0.5 wt/vol % solution of gelatin (Difco Laboratories) for 45 min at room temperature, followed by 15-min incubation with 0.5 wt/vol % glutaraldehyde (Merck, Germany) solution. The coated flasks were subsequently thoroughly rinsed with distilled water and dried overnight in a laminar flow chamber.

Immunocytochemistry of HSCs

To differentiate between SCs and fibroblasts, cultures of NCN61 and NCN68 were made on gelatin-coated coverslips (same coating procedure as described above for coating of the culture flasks), fixed with Cryofix® (Merck), rinsed three times with PBS, and incubated with antibodies appropriately diluted in PBS containing 0.1% bovine serum albumin and 1% normal goat serum (CLB, The Netherlands). To identify SCs, antibodies were added directed against S100 and glial fibrillary associated protein (Boehringer Mannheim Biochemica, Germany) in a dilution of 1:1000 and 1:500, respectively. For fibroblast identification, antibodies directed against fibroblasts (S5 clone), Thy 1.1 (Serotec, UK), and smooth muscle actin were used in a dilution of 1:100, 1:10,000, and 1:200, respectively. After overnight incubation at 4°C and 100% humidity, cultures were again rinsed three times with PBS and subsequently stained with goat anti-mouse/fluorescein isothiocyanate (Molecular Probes, The Netherlands) appropriately diluted in PBS containing 0.1% bovine serum albumin and 1% normal goat serum. After extensive rinsing with PBS, sections were mounted, dehydrated, and coverslipped with Fluoromount® (Merck) and viewed with a fluorescence microscope (Olympus, The Netherlands).

SC identity and functionality were further confirmed by testing for myelin production around cortical neurons as described elsewhere.[31]

HSC seeding

HSCs were collected from the gelatin-coated culture flasks by incubation for approximately 2 min at room temperature with a solution of 0.25% trypsin (Difco Laboratories) and 10 m*M* ethylenediaminetetraacetic acid in Dulbecco's modified Eagle's medium, followed by the addition of an equal amount of culture medium. A small cell sample was stained with True Blue (Janssen Chimica, Belgium) to evaluate cell viability. The cell number was estimated using a Bürker-Türk chamber and subsequently the cell suspension was centrifuged for 5 min at 1600 rpm. The cell pellet was washed with LAK culture medium and, after a second centrifugation step (5 min, 1600 rpm), the cells were resuspended in fresh culture medium to a final concentration of 2.8 × 10^3 cells/mL (the same seeding concentration was used in all studies). The cell suspension (500 μL aliquots) was added to the wells and incubated at 37°C in humidified air/5% CO_2. In proliferation experiments, the medium was refreshed three times per week. Glass slides (Menzel-Gläser) coated with gelatin were used as positive control (same coating procedure as described above for coating of the culture flasks).

HSC adhesion and proliferation

At the indicated times, cultures (in triplicate for each surface) were gently rinsed with PBS, fixed with Cryofix® and stained with 0.25 wt/vol % Coomassie blue solution in methanol/water/acetic acid (5:5:1). Subsequently, samples were fixed with an 8.8 wt/vol % trichloroacetic acid and 2.6 wt/vol % sulfosalicylic acid solution in a 23:77 vol % methanol/water mixture. Finally, the disks were coverslipped with Gur® (BDH, UK) and examined under the light microscope (Olympus) at 100× magnification. Cell numbers were determined by counting the cells present on the total area of the disks by direct microscopical observation. Morphology was assessed in terms of the size of the cells, the existence of clusters, and the presence of spaces between cells. Also, the relative homogeneity and overall morphology of the cells in culture were evaluated. Light micrographs of HSC cultures on the different surfaces were taken at the different evaluation time points (Nikon, Japan).

Statistical data analysis

Data are given as mean ± standard deviation (SD) and were analyzed using one-way analysis of variance, followed

TABLE I
Characterization of the Synthesized TMC and CL (co)polymers Used in the Preparation of the Polymer Disks

Polymer Composition TMC/CL (Mol Ratio)	$\bar{M}_n \times 10^{-5}$	$\bar{M}_w/\bar{M}_n$	T_g (°C)	T_m (°C)	w_c[a] (%)
100:0	3.4	1.7	−17	—	—
82:18	2.8	1.8	−29	—	—
10:90	1.4	1.8	−64	33	32
0:100	1.6	2.0	−68	55	45

[a]The mass fraction of crystallinity (w_c) was determined according to the expression: $w_c = \Delta H/\Delta H°$, where ΔH is the heat of fusion as determined by differential scanning calorimetry and $\Delta H°$ the heat of fusion of 100% crystalline poly(CL) reported to be 139.4 J/g.[43]

by Tukey's least significant differences multiple comparisons test. In the studies of HSC adhesion and proliferation on the polymer surfaces, the comparison between the cell counts on each polymer surface and gelatin at each time point was made by a two-sample *t* test (equal variances not assumed). Differences were considered statistically significant when $p < 0.05$. All calculations were performed using SPSS software for Windows (version 10.0) (SPSS, Chicago, IL).

RESULTS

Polymer characterization

The characteristics of the TMC and CL (co)polymers used in this study can be found in Table I. All synthesized materials have high molecular weight and range from amorphous rubbers in case of TMC-rich (co)polymers, to semicrystalline rubbers in case of the CL-rich (co)polymers.

Characterization of polymer films

In Table II, the equilibrium water uptake and the sessile drop and captive bubble contact angles of the different polymer films under study are presented. The water uptake is higher for the amorphous polymers. This can be explained by the absence of the denser crystalline domains. The contact angle determined by the sessile drop method (films in the dry state) slightly increased with the TMC content; nevertheless, all compositions yielded relatively hydrophobic polymer surfaces. The contact angle was also determined by the captive bubble method because an aqueous environment resembles the conditions in which the films were tested for SC adhesion and proliferation. For all polymer compositions, the contact angle on wet films was lower than the contact angle on dry films. An increase in TMC content had no effect on the contact angle values determined by the captive bubble method. Despite the described differences in water uptake and static contact angle in the dry and wet state between the polymers, all surfaces can be regarded as hydrophobic.

Scanning electron microscopic analysis of the films used for SC culture (data not shown) showed that poly(TMC) and 82:18 TMC–CL copolymer films have a very smooth surface. Poly(CL) and 10:90 TMC–CL copolymer film surfaces exhibited the spherulitic morphology characteristic of a semicrystalline material.

Purification and characterization of HSC cultures

Purification by the sequential explantation method resulted in cultures that stained almost exclusively with S100 and glial fibrillary associated protein antibodies, and only sporadically with fibroblast, Thy 1.1, and smooth muscle actin antibodies, indicating highly purified (95–98%) HSC cultures. Both cell lines (NCN61 and NCN 68) tested positive for myelin production around cortical neurons (data not shown).

Indicating high HSC viability, 99–100 % of the cells that were to be seeded stained with True Blue.

TABLE II
Wettability of the TMC and CL (Co)polymer Films

Polymer Composition TMC/CL (Mol Ratio)	Water Uptake[a] (wt %)	Sessile Drop Contact Angle (°)	Captive Bubble Contact Angle (°)
100:0	1.37 ± 0.15	73 ± 1	57 ± 2
82:18	1.24 ± 0.02	77 ± 1	52 ± 2
10:90	0.83 ± 0.03	80 ± 1	56 ± 2
0:100	0.51 ± 0.05	80 ± 1	62 ± 1

[a]Equilibrium water uptake, after conditioning in PBS, at 37°C for 24 h.

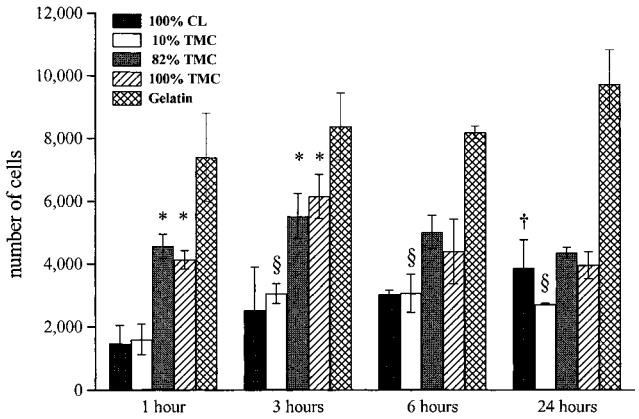

Figure 1. Total number of HSCs (NCN61) adhering to different TMC and CL (co)polymer films and gelatin at different time points. The data represent a mean ± SD of three independent measurements. The four (co)polymer compositions were compared among each other: *significantly different from poly(CL) and the 10:90 TMC–CL copolymer at the corresponding time point; §significantly different from the 10:90 TMC–CL copolymer at 1 h; †significantly different from poly(CL) at 1 h.

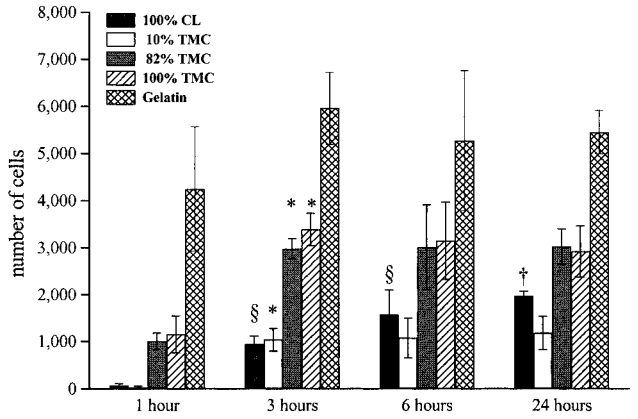

Figure 2. Total number of HSCs (NCN68) adhering to different TMC and CL (co)polymer films and gelatin at different time points. The data represent a mean ± SD of three independent measurements. The four (co)polymer compositions were compared among each other: *significantly different from corresponding polymer at 1 h; §significantly different from poly(CL) at 1 h; †significantly different from poly(CL) at 1 and 3 h.

HSC adhesion to TMC (co)polymers

HSC (NCN61) adhesion to TMC–CL copolymers and parent homopolymers was determined at 1, 3, 6, and 24 h after seeding (Fig. 1). Of all the polymer surfaces tested, poly(TMC) and 82:18 TMC–CL copolymer films showed the fastest and highest adhesion of SCs. One hour after seeding, the number of cells adhering to TMC-rich materials was higher compared with materials with lower TMC content. The number of cells that adhered to poly(CL) and the 10:90 TMC –CL copolymer showed an increase over time, reaching a plateau after 3 h of culture. In time, the number of cells attached to poly(TMC) and the 82:18 TMC–CL copolymer did not change. At all time points, the cell density was generally lower on CL-rich polymers than on TMC-rich materials. No increase in cell numbers was observed on gelatin over time. At the different time points, cell numbers on the polymer surfaces were significantly lower than those on gelatin [except at 1 h where there was no statistical difference between the number of cells on the TMC-rich (co)polymers and on gelatin].

To determine whether patient-to-patient variation would have an effect on HSC adhesion to the polymeric surfaces under study, cells derived from another patient (NCN 68) were seeded onto the TMC copolymer films (Fig. 2). Cell adhesion on the five different surfaces showed a similar trend as observed for the NCN61 culture. The number of cells adhering to the TMC-rich materials was generally higher compared with the number of cells adhering to materials with lower TMC content. However, cell adhesion on the polymers proceeded slower compared with the NCN61 culture. Cell density increased up to 3 h for the TMC-containing polymers and up to 6 h for poly(CL). Cell numbers on all tested polymer surfaces were significantly lower than those on gelatin at the different time points [except at 6 h where there was no statistical difference between the number of cells on the poly(TMC) films and on gelatin]. Cell numbers on gelatin also did not change over time, as observed with the NCN61 culture.

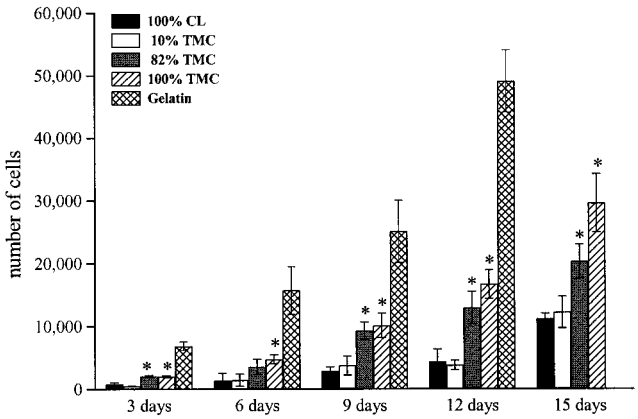

Figure 3. Total number of HSCs (NCN61) on different TMC and CL (co)polymer films and gelatin at different time points. At 15 days, the cell number on gelatin could not be determined accurately because of the very large number of cells covering the surface. The data represent a mean ± SD of three independent measurements. The four (co)polymer compositions were compared among each other: *significantly different from poly(CL) and the 10:90 TMC–CL copolymer at the corresponding time point.

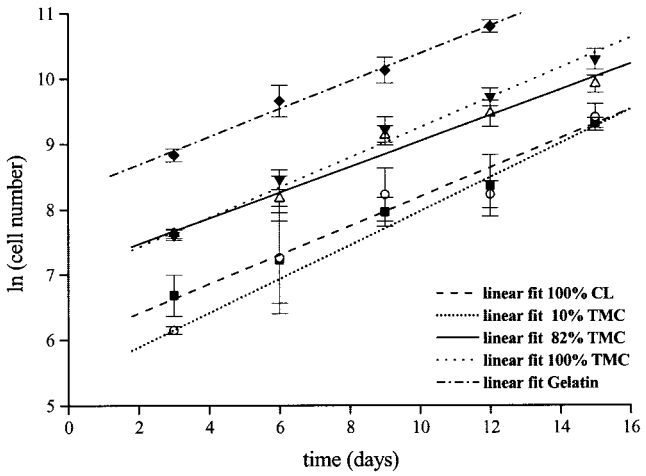

Figure 4. Natural logarithm of the average cell numbers observed on each surface versus time and correspondent linear fittings. The data represent a mean ± SD of three independent measurements. (■) 100% CL; (○) 10% TMC; (△) 82% TMC; (▼) 100% TMC; and (♦) gelatin.

HSC proliferation on TMC (co)polymers

In a separate study, HSC proliferation (NCN61) on the TMC–CL copolymers and parent homopolymer films was evaluated at 3, 6, 9, and 15 days of culture (Fig. 3). All surfaces tested showed significant cell proliferation between 3 and 15 days of culture.

In accordance to the observations at shorter culture times, the number of cells on poly(TMC) and the 82:18 TMC–CL copolymer was generally higher than on the polymers with higher CL content. Also in agreement with the higher initial cell adhesion, the total number of cells observed at all time points on gelatin was higher than on the polymeric surfaces.

The natural logarithm of the average cell number on each surface increases linearly as a function of time (Fig. 4). Therefore, despite differences in total cell numbers, HSCs displayed exponential cell growth when cultured on all the tested surfaces during the time scope of this study. From the slopes of the linear fittings, growth rates and doubling times were calculated for the HSCs on the different surfaces (Table III). There were no major differences between the growth rates and consequently doubling times of the cells cultured on the different polymer surfaces and gelatin. The cells divided approximately every 3 days.

HSC morphology on TMC (co)polymers

Figure 5 shows the appearance of HSCs (NCN61) on different TMC- and CL-based (co)polymer films and on gelatin at selected evaluation points. The time points 1 h, 24 h, and 9 days of culture were selected as indicative for the initial adhesion, the post-adhesion state, and advanced proliferation stage, respectively.

After 1 h of culture, >90% of the SCs present on poly(CL) and 10:90 TMC–CL copolymer films maintained their round shape ($14 < \text{diameter} < 60$ μm), but small lamellipodial extensions, the first signs of spreading, were present [Fig. 5(A1) and (B1)]. On the 82:18 TMC–CL copolymer and poly(TMC) films, only approximately 50% of the SCs maintained their round shape ($17 < \text{diameter} < 32$ μm) whereas the remainder of the cells were flattening, and exhibited lamellipodial extensions ($96 < \text{length} < 185$ μm) [Fig. 5(C1) and (D1)]. In the case of gelatin, all SCs were flattening after 1 h of culture, and exhibited many lamellipodial extensions ($42 < \text{length} < 172$ μm) [Fig. 5(E1)].

At 24 h of culture, both spindle-shaped and well-flattened SCs were observed on gelatin ($110 < \text{length} < 285$ μm) [Fig. 5(E2)]. On all polymeric surfaces, SCs formed clusters and were still not totally flattened. On the copolymers with high TMC content, cells tended to be more extended ($70 < \text{length} < 206$ μm) [Fig. 5(C2) and (D2)] than on films with high CL content where the cells were generally smaller ($68 < \text{length} < 128$ μm) [Fig. 5(A2) and (B2)].

After longer periods of culture, SCs were flattened on all surfaces and demonstrated a typical bi- or tripolar morphology and oval nuclei.[32] However, there were significant differences between the surfaces. On gelatin, a confluent packed layer of cells was observed after 9 days [Fig. 5(E3)]. Both spindle-shaped and elongated flattened SCs were observed. After 15 days (data not shown), the number of cells on gelatin continued to increase. The cells were well aligned and even more densely packed than at 9 days. On TMC-rich (co)polymers, SCs tended to be slightly elongated or spindle-shaped, and appeared more flattened than at initial culture times [Fig. 5(C3) and (D3)]. After 15 days of culture on these polymers, the cell layer was nearly confluent, but clusters of cells remained present. On the poly(CL) and the 10:90 TMC–CL copolymer, even at later stages of culture, the total SC numbers were lower than on the other surfaces tested, as previously mentioned [Fig. 5(A3) and (B3)]. After

TABLE III
Growth Rates and Doubling Times ± SD for HSCs (NCN61) Cultured on the Different TMC and CL (Co)polymer Films and on Gelatin

Surface	Growth Rate (Day^{-1})	Correlation Coefficient of Linear Fit (R)	Doubling Time (Days)
100% CL	0.22 ± 0.01	0.998	3.10 ± 0.08
10:90% TMC–CL	0.26 ± 0.02	0.994	2.66 ± 0.12
82:18% TMC–CL	0.20 ± 0.01	0.992	3.52 ± 0.18
100% TMC	0.23 ± 0.01	0.997	3.02 ± 0.10
Gelatin	0.22 ± 0.01	0.999	3.19 ± 0.07

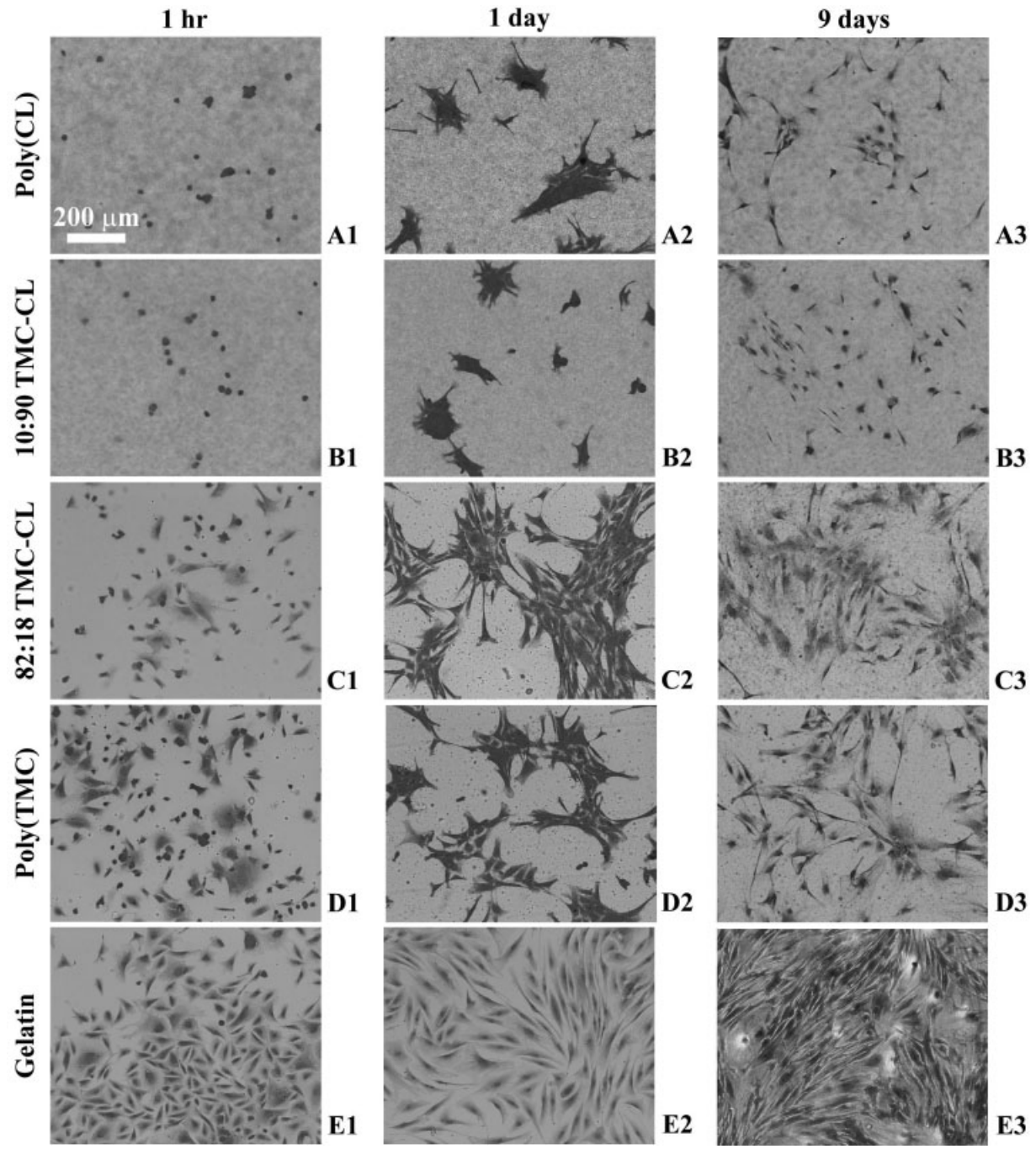

Figure 5. Light micrographs of HSCs (NCN61) on different surfaces at different time points (first column = 1 h, second column = 24 h, and third column = 9 days). (A1–A3) poly(CL); (B1–B3) 10:90 TMC–CL copolymer; (C1–C3) 82:18 TMC–CL copolymer; (D1–D3) poly(TMC); and (E1–E3) gelatin.

15 days, cultures were still not confluent and clusters of cells remained present. Furthermore, on these surfaces, the SCs had smaller dimensions ($37 < \text{length} < 201$ μm) than SCs cultured on gelatin ($91 < \text{length} < 303$ μm) or on the (co)polymers with high TMC content ($41 < \text{length} < 289$ μm), and were mainly spindle-shaped or with rounded morphology. Some flattened cells were also observed, but with thin and long cell protrusions.

HSC culture on fibronectin-coated TMC (co)polymers

Adhesion and proliferation of HSCs (NCN61) on fibronectin-coated polymer films were evaluated at 1, 6, and 24 h, and 3 and 9 days of culture, respectively. Gelatin surfaces (not coated with fibronectin) were used as control.

Both for short and long culture times, no significant

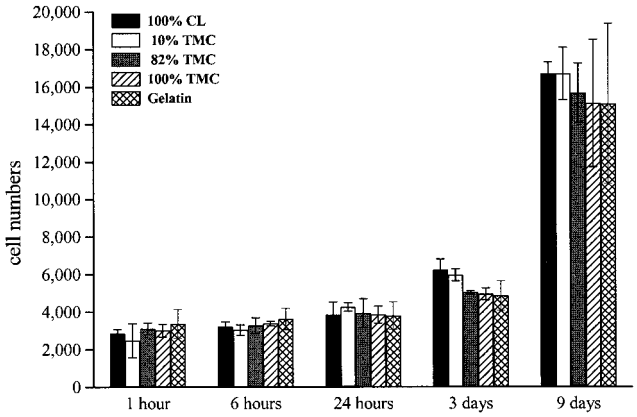

Figure 6. Total number of HSCs (NCN61) on different fibronectin-coated TMC and CL (co)polymer films and gelation at different culturing times. The data represent a mean ± SD of three independent measurements.

differences were observed between the total cell numbers on the five different surfaces (Fig. 6). Between 1 and 24 h of culturing, the number of cells adhering to the different surfaces did not significantly increase. In all cases, after the initial adhesion period, HSC numbers showed an exponential increase over time. Using the results obtained at 1, 3, and 9 days of culture, growth rates and doubling times for the HSCs cultured on the fibronectin-coated polymer films and gelatin were calculated (Table IV). There were no major differences between growth rates on the different surfaces; the cells divided approximately every 4 days.

In terms of morphology, the SCs appeared very similar on all surfaces at the different time points. After 1 h of culture, cells were still rather small ($52 < \text{length} < 169$ μm) but all were flattening. At 24 h of culture on all surfaces, cells were mainly flattened showing several lamellipodial extensions. However, in case of copolymers with high CL content, the cell extensions were thinner and longer than on the polymeric surfaces based on TMC-rich polymers or gelatin.

All cultures were confluent at 9 days with cells showing a more elongated ($100 < \text{length} < 279$ μm) and packed conformation. At this time, it was possible to observe both spindle-shaped and flattened cells in all cultures. Flattened cells on films of poly(CL) or on the 10:90 TMC–CL copolymer had thinner cell extensions appearing more like "ink-splashes" than like a "fried-egg" shape as observed for cells on the other (co)polymer surfaces and on gelatin.

DISCUSSION

The optimal way to incorporate SCs into an artificial nerve guide still needs to be determined. SCs can be seeded directly on the inner surface of the graft or after coating of the luminal graft surface with an adhesive substrate. Alternatively, the nerve guide can be filled with SCs in a supporting adhesive three-dimensional matrix, e.g., based on ECM proteins. In all cases, a prerequisite in the design of an artificial conduit with cultured SCs to be used in the clinic is the cell adhesion to the selected substrate and subsequent proliferation and functionality. In the present study, we evaluated the adhesion and proliferation of pure and viable HSC cultures on fibronectin-coated and noncoated TMC and CL (co)polymer films.

Cell adhesion and proliferation occurred on all tested polymer surfaces. However, for both primary HSC lines tested, a faster and higher cell adhesion was observed on films with higher TMC content. Cell attachment on the polymeric surfaces was lower and slower than on gelatin (positive control). The determined number of cells that had attached to the surfaces under study was higher than the estimated number of seeded cells (except in the study of the proliferation of HSC on noncoated polymeric surfaces). In contrast with the cell number determination by direct observation, the estimation of the cell concentration in the cell suspension to be seeded by means of the Bürker-Türk chamber method can be hampered by the agglomeration of the cells after trypsinization. Therefore, the observed differences can be explained by an underestimation of the number of cells initially seeded. Despite differences in cell adhesion, exponential cell growth was observed on all polymer films as well as on gelatin. The growth rates were similar on all surfaces with cell numbers doubling approximately every 3 days. The growth rates previously reported for HSCs cultured in the presence of mitogens vary between 3–4 days,[33] similar to the ones observed in our study, to 1–2 weeks.[34] Such differences in the growth rates may arise from isolation of the cells from different donors or donor sites and the use of different culture conditions such as cell culture substrate, culture media composition, and seeding densities.

When proliferating on the polymer films and on

TABLE IV
Growth Rates and Doubling Times ± SD for HSCs (NCN61) Cultured on the Different TMC and CL (Co)polymer Films Coated with Fibronectin and on Gelatin

Surface	Growth Rate (Day^{-1})	Correlation Coefficient of Linear Fit (R)	Doubling Time (Days)
100% CL	0.17 ± 0.01	0.998	4.06 ± 0.16
10:90% TMC–CL	0.17 ± 0.01	0.999	4.05 ± 0.02
82:18% TMC–CL	0.19 ± 0.01	0.998	3.70 ± 0.15
100% TMC	0.17 ± 0.02	0.991	4.09 ± 0.39
Gelatin	0.17 ± 0.02	0.995	3.97 ± 0.29

gelatin, cells presented the typical bi- or tripolar morphology.[32] However, on the polymer films, cells tended to form clusters, and on the CL-rich materials in particular, at all time points, the cells were smaller and had fewer lamellipodial extensions.

The results demonstrate that the surface properties of the TMC-based polymers have an effect on the initial adhesion and overall morphology of HSCs. In terms of the substrate wettability, TMC-rich films were found to be slightly less hydrophobic than CL-rich films. However, in view of the small differences observed, all polymer surfaces can be considered equally hydrophobic. Therefore, dissimilarities in cell behavior cannot be directly correlated to the surface wettability. With the increase of CL content in the polymer, the ratio of ester/carbonate units increases as well as the number of crystallizable units per polymer chain. CL-rich (co)polymer films are semicrystalline, featuring the characteristic spherulite morphology, in contrast to the amorphous and more flexible TMC-rich (co)polymers. Chemical composition, polymer morphology (crystallinity), and mechanical characteristics may affect the polymer surface properties. Ultimately, this may not only influence the nature and the amount of protein adsorption from serum containing medium onto the polymer film, but can also regulate conformational changes of the adsorbed protein, thus indirectly controlling cell adhesion and protein-mediated cell functions.[35] ECM proteins in the culture medium, like fibronectin, contain RGD amino acid sequences that can be recognized by integrin receptors present in the cell membrane of the SC.[36,37] This interaction causes the SC to attach to the surface and promotes a series of other events such as cell spreading and cytoskeletal reorganization. The effect of polymer composition on the adsorption of proteins present in the culture medium onto the prepared TMC and CL (co)polymer films is currently being investigated by means of surface plasmon resonance, an optical technique that allows the investigation of dynamic surface events *in situ* in real time.[38]

Although the mechanism mediating HSC behavior on the different polymers is not yet fully understood, the results described so far show that all materials allow SC adhesion and proliferation independently of the donor source, and that HSCs proliferate at comparable growth rates. Therefore, TMC- and CL-based (co)polymers can in principle be used for the preparation of artificial nerve grafts. If cells are to be seeded directly on the inner surface of the graft, higher cell numbers may be reached in shorter periods by increasing the initial cell seeding densities.

SCs can also be seeded onto the luminal surface of a nerve graft that has been precoated with an adhesive substrate. ECM proteins such as fibronectin, laminin, or collagen stimulate the outgrowth of neurites and improve nerve regeneration over large nerve gaps.[39–41] In this study, fibronectin was selected as a coating because it is known to promote cell-substratum adhesion under a variety of conditions. The adhesion and proliferation of HSCs on different ECM protein coatings, including fibronectin, was evaluated in a separate study.[42] When the TMC- and CL-based polymer surfaces were coated with fibronectin before culture, no significant differences in cell behavior between the polymer surfaces and gelatin were found. HSC adhesion was improved to levels comparable to gelatin and SC morphology was similar as observed on gelatin. Surface modification with fibronectin apparently masks the polymer surface properties and provides optimal HSC adhesion and proliferation. Exponential cell growth was also observed on the fibronectin-coated polymer substrates. The growth rates were similar on all surfaces, with cell numbers now doubling approximately every 4 days. Because more cells adhere to the polymer surfaces as a result of fibronectin coating, the use of ECM protein-coated nerve guides can reduce the required number of HSCs needed for seeding.

A. P. Pêgo acknowledges the PRAXIS XXI programme (Portuguese Foundation for Science and Technology) for her research grant. The authors thank M. Smithers for performing the scanning electron microscopy studies.

References

1. Merle M, Dellon AL, Campbell JN, Chang PS. Complications from silicon-polymer intubulation of nerves. Microsurgery 1989;10:130–133.
2. Madison R, Sidman RL, Nyilas E, Chiu T-H, Greatorex D. Nontoxic nerve guide tubes support neovascular growth in transected rat optic nerve. Exp Neurol 1984;86:448–461.
3. Kiyotani T, Teramachi M, Takimoto Y, Nakamura T, Shimizu Y, Endo K. Nerve regeneration across a 25-mm gap bridged by a polyglycolic acid-collagen tube: A histological and electrophysiological evaluation of regenerated nerves. Brain Res 1996; 740:66–74.
4. den Dunnen WFA, van der Lei B, Robinson PH, Holwerda A, Pennings AJ, Schakenraad JM. Biological performance of a degradable poly(DL-lactide-ecaprolactone) nerve guide: Influence of tube dimensions. J Biomed Mater Res 1995;29:757–766.
5. Langone F, Lora S, Veronese FM, Caliceti P, Parnigotto PP, Valenti F, Palma G. Peripheral nerve repair using a poly(organo) phosphazene tubular prosthesis. Biomaterials 1995;16:347–353.
6. Aldini NN, Perego G, Cella GD, Maltarello MC, Fini M, Rocca M, Giardino R. Effectiveness of a bioabsorbable conduit in the repair of peripheral nerves. Biomaterials 1996;17:959–962.
7. Chamberlain LJ, Yannas IV, Hsu H-P, Spector M. Histological response to a fully degradable collagen device implanted in a gap in the rat sciatic nerve. Tissue Eng 1997;3:353–362.
8. Mackinnon SE, Dellon AL. A study of nerve regeneration across synthetic (Maxon) and biologic (collagen) nerve conduits for nerve gaps up to 5 cm in the primate. J Reconstr Microsurg 1990;6:117–121.
9. Rodriguez FJ, Gomez N, Perego G, Navarro X. Highly permeable polylactide-caprolactone nerve guides enhance peripheral

nerve regeneration through long gaps. Biomaterials 1999;20: 1489–1500.
10. den Dunnen WF, Meek MF, Grijpma DW, Robinson PH, Schakenraad JM. *In vivo* and *in vitro* degradation of poly[50/50 (85/15 L/D)LA/ϵ-CL], and the implications for the use in nerve reconstruction. J Biomed Mater Res 2000;51:575–585.
11. Bryan DJ, Holway AH, Wang KK, Silva AE, Trantolo DJ, Wise D, Summerhayes IC. Influence of glial growth factor and Schwann cells in a bioresorbable guidance channel on peripheral nerve regeneration. Tissue Eng 2000;6:129–138.
12. Guénard V, Kleitman N, Morrissey TK, Bunge RP, Aebischer P. Syngeneic Schwann cells derived from adult nerves seeded in semipermeable guidance channels enhance peripheral nerve regeneration. J Neurosci 1992;12:3310–3320.
13. Keeley R, Atagi T, Sabelman E, Padilla J, Kadlcik P, Agras J, Eng L, Wiedman T-W, Nguyen K, Sudekum A, Rosen J. Synthetic nerve graft containing collagen and synthetic Schwann cells improves functional, electrophysiological, and histological parameters of peripheral nerve regeneration. Restor Neurol Neurosci 1993;5:353–366.
14. Kim DH, Connolly SE, Kline DG, Voorhies RM, Smith A, Powell M, Yoes T, Daniloff JK. Labeled Schwann cell transplants versus sural nerve grafts in nerve repair. J Neurosurg 1994;80:254–260.
15. Bryan DJ, Wang RR, Chakalis-Haley DP. Effect of Schwann cells in the enhancement of peripheral-nerve regeneration. J Reconstr Microsurg 1996;12:439–446.
16. Ansselin AD, Fink T, Davey DF. Peripheral nerve regeneration through nerve guides seeded with adult Schwann cells. Neuropathol Appl Neurobiol 1997;23:387–398.
17. Rodriguez FJ, Verdu E, Ceballos D, Navarro X. Nerve guides seeded with autologous Schwann cells improve nerve regeneration. Exp Neurol 2000;161:571–584.
18. Terenghi G. Peripheral nerve injury and regeneration. Histol Histopathol 1995;10:709–718.
19. Son Y-J, Thompson WJ. Schwann cell processes guide regeneration of peripheral axons. Neuron 1995;14:125–132.
20. Fu SY, Gordon T. The cellular and molecular basis of peripheral nerve regeneration. Mol Neurobiol 1997;14:67–116.
21. Frostick SP, Yin Q, Kemp GJ. Schwann cells, neurotrophic factors, and peripheral nerve regeneration. Microsurgery 1998; 18:397–405.
22. Pêgo AP, Poot AA, Grijpma DW, Feijen J. Copolymers of trimethylene carbonate and ϵ-caprolactone for porous nerve guides: Synthesis and properties. J Biomater Sci Polym Ed 2001;12:35–53.
23. Pêgo AP, Poot AA, Grijpma DW, Feijen J. *In vitro* degradation of trimethylene carbonate based (co)polymers. Macromol Biosci 2002;2:411–419.
24. Pêgo AP, van Luyn MJA, Brouwer LA, van Wachem PB, Poot AA, Grijpma DW, Feijen J. *In vivo* behavior of poly(1,3-trimethylene carbonate) and copolymers of 1,3-trimethylene carbonate with D,L-lactide or ϵ-caprolactone: Degradation and tissue response. 2002. Submitted for publication.
25. Steuer H, Fadale R, Müller E, Müller HW, Planck H, Schlosshauer B. Biohybride nerve guide for regeneration: Degradable polylactide fibers coated with rat Schwann cells. Neurosci Lett 1999;277:165–168.
26. Hadlock T, Sundback C, Hunter D, Cheney M, Vacanti JP. A polymer foam conduit seeded with Schwann cells promotes guided peripheral nerve regeneration. Tissue Eng 2000;6:119–127.
27. Hadlock TA, Sundback CA, Hunter DA, Vacanti JP, Cheney ML. A new artificial nerve graft containing rolled Schwann cell monolayers. Microsurgery 2001;21:96–101.
28. Mosahebi A, Simon M, Wiberg M, Terenghi G. A novel use of alginate hydrogel as Schwann cell matrix. Tissue Eng 2001;7: 525–534.
29. Morrissey TK, Kleitman N, Bunge RP. Isolation and functional characterization of Schwann cells derived from adult peripheral nerve. J Neurosci 1991;11:2433–2442.
30. Lamers CH, van de Griend RJ, Braakman E, Ronteltap CP, Benard J, Stoter G, Gratama JW, Bolhuis RL. Optimization of culture conditions for activation and large-scale expansion of human T lymphocytes for bispecific antibody-directed cellular immunotherapy. Int J Cancer 1992;51:973–979.
31. Marani E. Culturing neurons and Schwann cells. Abstracts XIV National Congress Bulgarian Anatomical Society. Eur J Morphol. Forthcoming.
32. Levi AD. Characterization of the technique involved in isolating Schwann cells from adult human peripheral nerve. J Neurosci Methods 1996;68:21–26.
33. Casella GT, Wieser R, Bunge RP, Margitich IS, Katz J, Olson L, Wood PM. Density dependent regulation of human Schwann cell proliferation. Glia 2000;30:165–177.
34. Spierings E, de Boer T, Wieles B, Adams LB, Marani E, Ottenhoff TH. Mycobacterium leprae-specific, HLA class II-restricted killing of human Schwann cells by CD4(+) Th1 cells: A novel immunopathogenetic mechanism of nerve damage in leprosy. J Immunol 2001;166:5883–5888.
35. Garcia AJ, Vega MD, Boettiger D. Modulation of cell proliferation and differentiation through substrate-dependent changes in fibronectin conformation. Mol Biol Cell 1999;10:785–798.
36. Chernousov MA, Carey DJ. Schwann cell extracellular matrix molecules and their receptors. Histol Histopathol 2000;15:593–601.
37. Previtali SC, Feltri ML, Archelos JJ, Quattrini A, Wrabetz L, Hartung H. Role of integrins in the peripheral nervous system. Prog Neurobiol 2001;64:35–49.
38. Green RJ, Frazier RA, Shakesheff KM, Davies MC, Roberts CJ, Tendler SJB. Surface plasmon resonance analysis of dynamic biological interactions with biomaterials. Biomaterials 2000;21: 1823–1835.
39. Madison RD, Da Silva CF, Dikkes P. Entubulation repair with protein additives increases the maximum nerve gap distance successfully bridged with tubular prostheses. Brain Res 1988; 447:325–334.
40. Woolley AL, Hollowell JP, Rich KM. Fibronectin-laminin combination enhances peripheral nerve regeneration across long gaps. Otolaryngol Head Neck Surg 1990;103:509–518.
41. Bailey SB, Eichler ME, Villadiego A, Rich KM. The influence of fibronectin and laminin during Schwann cell migration and peripheral nerve regeneration through silicon chambers. J Neurocytol 1993;22:176–184.
42. Vleggeert-Lankamp CLAM, Pêgo AP, Deenen M, Lakke EAJF, Poot AA, Grijpma DW, Feijen J, Marani E. Human Schwann cell proliferation on coatings. Biomaterials. Forthcoming.
43. Crescenzi V, Manzini G, Calzolari G, Borri C. Thermodynamics of fusion of poly-β-propiolactone and poly-ϵ-caprolactone. Comparative analysis of the melting of aliphatic polylactone and polyester chains. Eur Polym J 1972;8:449–463.